International Journal of Electrical and Computer Engineering (IJECE)
Vol. 10, No. 4, August 2020, pp. 4015~4022
ISSN: 2088-8708, DOI: 10.11591/ijece.v10i4.pp4015-4022

Dual-layer remote phosphor structure: a novel technique to enhance the color quality scale and luminous flux of WLEDs

Phung Ton That[1], Thuc Minh Bui[2], Nguyen Thi Phuong Loan[3], Phan Xuan Le[4], Nguyen Doan Quoc Anh[5], Le Van Tho[6]
[1]Faculty of Electronics Technology, Industrial University of Ho Chi Minh City, Vietnam
[2]Faculty of Electrical and Electronics Engineering, Nha Trang University, Vietnam
[3]Faculty of Fundamental 2, Posts and Telecommunications Institute of Technology, Vietnam
[4]Faculty of Electrical and Electronics Engineering, HCMC University of Food Industry, Vietnam
[5]Power System Optimization Research Group, Faculty of Electrical and Electronics Engineering, Ton Duc Thang University, Vietnam
[6]Institute of Tropical Biology, Vietnam Academy of Science and Technology, Vietnam

Article Info

Article history:

Received Sep 9, 2019
Revised Feb 14, 2020
Accepted Feb 24, 2020

Keywords:

Color rendering index
Luminous flux
Dual-layer phosphor
Mie-scattering theory
WLEDs

ABSTRACT

The effects of red light-emitting phosphor CaMgSi2O6:Eu2+,Mn2+ on the optical properties of single-layer remote phosphor structure (SRPS) and dual-layer remote phosphor structure (DRPS) are the focus of this study. The differences in color quality and luminous flux (LF) of white light-emitting diodes (WLEDs) between these two structures are also revealed and demonstrated based on the Mie theory. SRPS consists of one mixed phosphor layer betweenCaMgSi2O6:Eu2+,Mn2+ andYAG:Ce3+particles, while DRPS includes two separated layers: red phosphor layer and yellow phosphor layer. In this work, 5% SiO2 is added into the phosphor layers to increase scattering abilities. Discrepancies in structures greatly affect the optical characteristics of WLEDs. The results showed that the color rendering index (CRI) increased with the concentration in both structures with nearly equal values. Meanwhile, color quality scale (CQS) of DPRS is 74 at ACCTs ranging from 5600K to 8500K, higher than CQS of SRPS which is only 71 at 8500K. In addition, the luminous flux of DRPS is significantly higher than SRPS at 2% -14% of CaMgSi2O6:Eu2+,Mn2+. In summary, DRPS is better for color quality and lumen outputin comparison to SRPS and adding the right amount of red phosphor can enhance CQS and LF.

Corresponding Author:

Nguyen Doan Quoc Anh,
Faculty of Electrical and Electronics Engineering,
Ton Duc Thang University,
No. 19 Nguyen Huu Tho Street, Tan Phong Ward, District 7, Ho Chi Minh City, Vietnam.
Email: nguyendoanquocanh@tdtu.edu.vn

1. INTRODUCTION

The light-emitting diodes that eject white light (WLEDs) are one of the most commonly used lighting solution in the lighting and display systems industry for their unique properties, including reliability, luminous efficiency, and energy efficiency, which is likely to replace older lighting techniques in the future [1-4]. However, there aremajor changes in WLEDs that can be made to reach the full potential including phosphor conversion and luminous efficiency [5-6], as well as improving color purity and price competitiveness against incandescent and fluorescent lamps [7-10]. In previous studies, quantum efficiency was enhanced using a phosphors synthesis methodology called exploiting flux [11-14] and inventing a novel phosphor. Researchers have recently adjusted the configuration of LED tools by modifying the gap between the phosphor material and the lighting emitting chip, creating a new type of LED named remote-type LED

which works on the scattered photon extraction concept and improves the quantum efficiency of WLED up to 60% by boosting the back-scattered photons extraction efficiency [15].

Enhancing brightness and luminous efficiency also relies upon the color quality. A notable method that usually appliedin WLED production is emerging the blue light of InGaN LED chip with the yellow green light from a phosphor; however, the red light lack these elements [16]. Therefore, it is essential that red phosphor and green-yellow phosphor are combined in order to yield better color quality. The process that produce the compound of these two phosphors, however, damages the obtained light from emission process due to a part of light emitted from one phosphor is reabsorbed by another causing an overlap of phosphor spectrawhich leads tolow color quality [17]. A possible solution is stacking the layers of phosphor materials in the order of red phosphor layer below the green one to enhance the efficiency. This pattern suggests that the layer of red phosphor can reduce the reabsorption of light from green phosphor if placed directly above the chip [18]. Nevertheless, stacked phosphor layers model cannot be re-implemented for copyright and patents reasons to avoid risks related to law violations, [8], which forces us to look for a new method named phosphor-in-glass (PiG) to improve the chromatic quality and heat performance in WLED configuration with remote phosphor layers [19-20]. Not only does PiG benefit the luminous efficacy and thermal stability of WLEDs but it also offers color quality advantages that very few research papers have mentioned or proved. In this study, optical properties such as luminous efficiency and color quality of WLEDs are improved by utilizing a new technique called dual-layer remote phosphor structure (DRPS). Besides, the comparison of optical characteristics between SRPS (single remote phosphor structure) and DRPS is also clearly presented and demonstrated based on Mie scattering theory.

2. DETAIL OF SIMUALTION

2.1. Simulation of SRPS and DRPS

As can be seen from Figure 1(a), the WLED simulation with remote phosphor structuresthat have the average CCTs of 5600 K, 6600 K,7000 K, 7700 K, and 8500 Kwas made from a commercial software utilizing the Monte Carlo ray-tracing method, the LightTools 8.1.0. Figure 1(b) depicted the 3-D simulation physical model of WLEDs used to perform optical simulations of remote package WLEDs. SRPS consists of a single phosphor layer in which $CaMgSi_2O_6:Eu^{2+},Mn^{2+}$ are mixed with $YAG:Ce^{3+}$ compound as illustrated in Figure 1 (c). On the other hand, according to Figure 1 (d), DRPS includes two separated layers of red phosphor and yellow phosphor.This realistic model of WLEDs consists ofan 8 mm long reflector at the sole, 2.07 mm high, and 9.85 mm long at its top surface. As depicted in Figure 1(d), the thickness for each layer of remote phosphor is 0.08 mm with nine LED chips, each of them has 1.16 W radiant power at 455 nm wavelength, a square sole of 1.14 mm, and is 0.15 mm high bounded to the spaces at the botton of the reflector.When the SiO_2 concentration in the mixture of phosphor is fixed at 5%, the concentration of CaMg phosphor climbs ceaselessly from 2% to 30%. However, the average CCT values are stabilized with the modification of $YAG:Ce^{3+}$ wt.

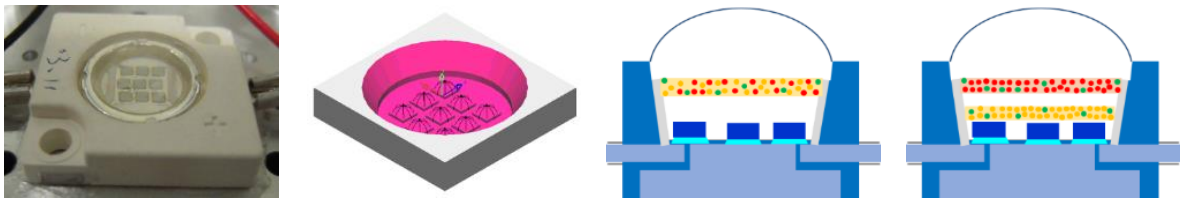

(a) (b) (c) (d)

Figure 1. a) Photograph of WLEDs sample, (b) Simulation of the WLEDs using LightTools program, (c) Illustration of SRPS with SiO_2 (green) and $CaMgSi_2O_6:Eu^{2+},Mn^{2+}$ (red) in $YAG:Ce^{3+}$ compound (yellow), (d) Illustration of DRPS with SiO_2 in $CaMgSi_2O_6:Eu^{2+},Mn^{2+}$ compound and $YAG:Ce^{3+}$ compound.

Next, the LightTools 8.5.0 software is applied to simulate the particles properties of SiO_2 and $CaMgSi_2O_6:Eu^{2+},Mn^{2+}$. The refractive index of SiO_2 and $CaMgSi_2O_6:Eu^{2+},Mn^{2+}$ phosphor is 1.54 and 1.80 respectively. The SiO_2 particles have spherical shape with a 3 µm average radius in the Mie simulation while the $YAG:Ce^{3+}$ phosphor particles have an average radius of 7.25 µm with consistent 1.38 refractive index at every wavelengths, and the refractive index for the silicone glue is 1.5. To keep the average CCT value steady, it is vital to vary the diffusional particle density in the direction of increasing the weight of the diffuses to increase their percentage while lessening the weight of $YAG:Ce^{3+}$ phosphor to retain the balance.

2.2. Preparation of $CaMgSi_2O_6:Eu^{2+},Mn^{2+}$ phosphor

Ordinarily, red-emitting phosphor $CaMgSi_2O_6:Eu^{2+},Mn^{2+}$ is suitable for high loading and long lifetime fluorescent lamps because of the outstanding properties in quantum efficiency or chemical and thermal stability [11]. The $CaMgSi_2O_6:Eu^{2+},Mn^{2+}$ composition,which is supposedly a substance that can enhance the luminous efficacy of WLEDs,is created through the chemical processes between different materials such as CaO, MgO, SiO_2, Eu_2O_3, $MnCO_3$ and NH_4Cl. The $CaMgSi_2O_6:Eu^{2+},Mn^{2+}$ phosphor composition is calculated in detail as can be seen from Table 1. The fabrication of $CaMgSi_2O_6:Eu^{2+},Mn^{2+}$ must be taken in order of six separate steps: mixing, drying, firing twice, washing and drying again to get the best result, each of them plays an essential role and closely relates to the preceding step(s). This order is presented specifically as follows: (1) Mix the materials by slurrying them in methanol with the focus on soaking with a few cubic centimeters water; (2) Dry the mixture in the air until it completely gets drained; (3) Fire the dried materials in capped quartz tubes under the condition of N2 at 1000ºC within an hour; (4) Fire this compound again in capped quartz tubes n an hour but with CO at 1150ºC. (5) Collect and wash with water to remove residue and dust. (6) Wait until the materials dry and we achieve $CaMgSi_2O_6:Eu^{2+},Mn^{2+}$.

Table 1. Composition of the red-emitting $CaMgSi_2O_6:Eu^{2+},Mn^{2+}$phosphor

Ingredient	Mole (%)	By weight (g)	Molar mass (g/mol)	Mole (mol)	Ions	Mole (mol)	Mole (%)
CaO	26,659	64	56.0774	1.141	Ca^{2+}	1.141	0.106
MgO	23.183	40	40.304	0.992	Mg^{2+}	0.992	0.092
SiO_2	48.989	126	60.08	2.097	Si^{4+}	2.097	0.195
Eu_2O_3	0.234	3.5	351.926	0.01	O^{2-}	6.478	0.601
$MnCO_3$	0.935	4.6	114.9469	0.04	Eu^{2+}	0.02	0.002
NH_4Cl	--	21.4	53.49	--	Mn^{2+}	0.04	0.004

3. SCATTERING COMPUTATION

The scattering coefficient $\mu_{sca}(\lambda)$, anisotropy factor $g(\lambda)$, and reduced scattering coefficient $\delta_{sca}(\lambda)$according to Mie theory [21-25] can be defined by applying expressions (1-3):

$$\mu_{sca}(\lambda) = \int N(r) C_{sca}(\lambda, r) dr \tag{1}$$

$$g(\lambda) = 2\pi \int_{-1}^{1} \int p(\theta, \lambda, r) f(r) \cos\theta d \cos\theta dr \tag{2}$$

$$\delta_{sca} = \mu_{sca}(1-g) \tag{3}$$

where N(r) indicates the density of distributed diffusional particles (mm^3), C_{sca} is the scattering cross sections (mm^2), $p(\theta,\lambda,r)$ is the phase function, λ is the light wavelength (nm), r is diffusional particles radius (μm), θ is the scattering angle (°C), and f(r) is the function describe the diffusor distribution of size in the phosphor layer, which can be calculated as follows:

$$f(r) = f_{dif}(r) + f_{phos}(r) \tag{4}$$

$$\begin{aligned} N(r) &= N_{dif}(r) + N_{phos}(r) \\ &= K_N.[f_{dif}(r) + f_{phos}(r)] \end{aligned} \tag{5}$$

The function N(r) are compiled by the density ofdiffusive particle $N_{dif}(r)$ and phosphor particle $N_{phos}(r)$. $f_{dif}(r)$ and $f_{phos}(r)$ are functions fordiffusor and phosphor particle size distribution. K_N is the diffusor unitsin one diffusor concentration and is defined by:

$$c = K_N \int M(r) dr \tag{6}$$

where M(r) is the diffusive unit spatial distribution of mass, proposed by equation:

$$M(r) = \frac{4}{3}\pi r^3[\rho_{dif}\, f_{dif}(r) + \rho_{phos}\, f_{phos}(r)] \tag{7}$$

$\rho_{diff}(r)$ and $\rho_{phos}(r)$describethe diffusor and phosphor density.

In Mie-scattering theory, C_{sca} can be achieved as a results of the equation below:

$$C_{sca} = \frac{2\pi}{k^2}\sum_{0}^{\infty}(2n-1)(|a_n|^2 + |b_n|^2) \tag{8}$$

where $k = 2\pi/\lambda$, and a_n and b_n are estimated by:

$$a_n(x,m) = \frac{\psi_n'(mx)\psi_n(x) - \mathrm{m}\psi_n(mx)\psi_n'(x)}{\psi_n'(mx)\xi_n(x) - \mathrm{m}\psi_n(mx)\xi_n'(x)} \tag{9}$$

$$b_n(x,m) = \frac{m\psi_n'(mx)\psi_n(x) - \psi_n(mx)\psi_n'(x)}{m\psi_n'(mx)\xi_n(x) - \psi_n(mx)\xi_n'(x)} \tag{10}$$

Which have the refractive index$x = k.rm$, andRiccati - Bessel function $\psi_n(x)$ and $\xi_n(x)$. It can be seen from Figure 2 that the scattering coefficients at453 nm, 555 nm, and 680 nm wavelengthsincrease dependently on the $CaMgSi_2O_6:Eu^{2+},Mn^{2+}$ phosphor concentration. The scattering effects of $CaMgSi_2O_6:Eu^{2+},Mn^{2+}$ and SiO_2 particles cause considerable influence on RP-WLEDs. Particularly, the red light from $CaMgSi_2O_6:Eu^{2+},Mn^{2+}$ has better absorbing capability than the light radiation of LED and therefor, the will be abundant red light which can be used to compensate for deficiency in RP-WLEDs. Furthermore, 5% wt. of SiO_2 was added to enhance the scattered light, resulting in a rise assimilated light of pc-LEDs, which is the reason why $CaMgSi_2O_6:Eu^{2+},Mn^{2+}$ and SiO_2 particles are utilized to yield white LEDs with better color quality. Next, the anisotropy factor of $CaMgSi_2O_6:Eu^{2+},Mn^{2+}$ particles for wavelengths of 453nm, 555nm, and 680nm was presented in Figure 3, which indicates the anisotropy factor values at 680nm wavelength increases in comparison to 555nm values. In comparison with other wavelengths, the anisotropy factor values obtained at 453nm wavelength is the highest, which means $CaMgSi_2O_6:Eu^{2+},Mn^{2+}$ particles are favorable to the color homogeneity of remote phosphor WLEDs.

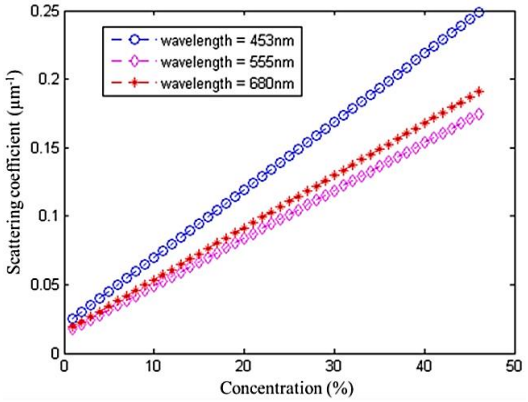

Figure 2. Scattering coefficients of $CaMgSi_2O_6:Eu^{2+},Mn^{2+}$ of 453 nm, 555 nm, and 680 nm wavelengths

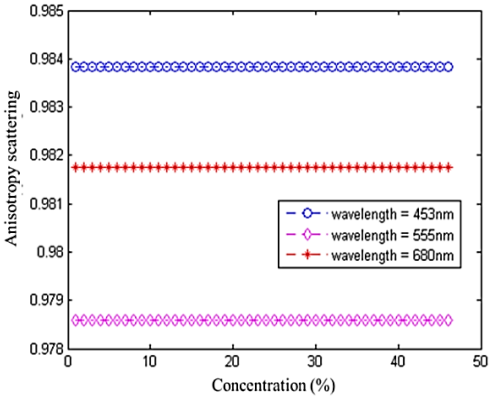

Figure 3. Anisotropy scattering of $CaMgSi_2O_6:Eu^{2+},Mn^{2+}$of 453 nm, 555 nm, and 680 nm wavelengths

The refractive index of silicone (n_{sil}) in SRPS and DRPS is 1.53 while n_{phos} is the refractive index of the phosphor particles. Therefore, the relative refractive values of diffusive particles (m_{dif}) and phosphor (m_{phos}) in the silicone can be computed from $m_{dif} = n_{dif} / n_{sil}$ and $m_{phos} = n_{phos} / n_{sil}$. Then the phase function is expressed as follows:

$$p(\theta,\lambda,r)=\frac{4\pi\beta(\theta,\lambda,r)}{k^2C_{sca}(\lambda,r)} \tag{11}$$

where $\beta(\theta,\lambda,r)$, $S_1(\theta)$ and $S_2(\theta)$ are the angular scattering amplitudes calculated by the following equations:

$$\beta(\theta,\lambda,r)=\frac{1}{2}[|S_1(\theta)|^2+|S_2(\theta)|^2] \tag{12}$$

$$S_1=\sum_{n=1}^{\infty}\frac{2n+1}{n(n+1)}\begin{bmatrix}a_n(x,m)\pi_n(\cos\theta)\\+b_n(x,m)\tau_n(\cos\theta)\end{bmatrix} \tag{13}$$

$$S_2=\sum_{n=1}^{\infty}\frac{2n+1}{n(n+1)}\begin{bmatrix}a_n(x,m)\tau_n(\cos\theta)\\+b_n(x,m)\pi_n(\cos\theta)\end{bmatrix} \tag{14}$$

4. RESULTS AND DISCUSSION

Figure 4 showed that the reduction in scattering coefficient of $CaMgSi_2O_6:Eu^{2+},Mn^{2+}$at 453nm, 555nm, and 680nm wavelengths are nearly equal, creating the scattering stability of $CaMgSi_2O_6:Eu^{2+},Mn^{2+}$, which is beneficial for the chromatic performance of remote phosphor WLEDs. The angular scattering amplitudes of $CaMgSi_2O_6:Eu^{2+},Mn^{2+}$ are also computed by MATLAB program after that. According to the obtained results, $CaMgSi_2O_6:Eu^{2+},Mn^{2+}$ particles are greatly advantageous to the blue-light scattering. As known, a large amount in blue light can lessen the effect of yellow ring. Meanwhile, $CaMgSi_2O_6:Eu^{2+},Mn^{2+}$ particles not only compensate to the red-light but also to the blue-light, as shown in angular scattering amplitudes within Figure 5. These calculations demonstrating the results from Figure 6 to Figure 8.

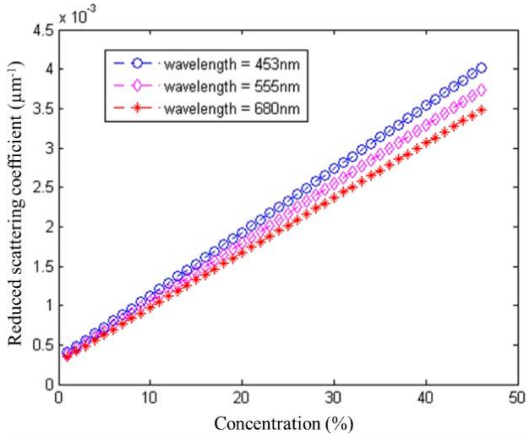

Figure 4. Reduced scattering coefficient of $CaMgSi_2O_6:Eu^{2+},Mn^{2+}$of 453nm, 555nm, and 680nm wavelengths

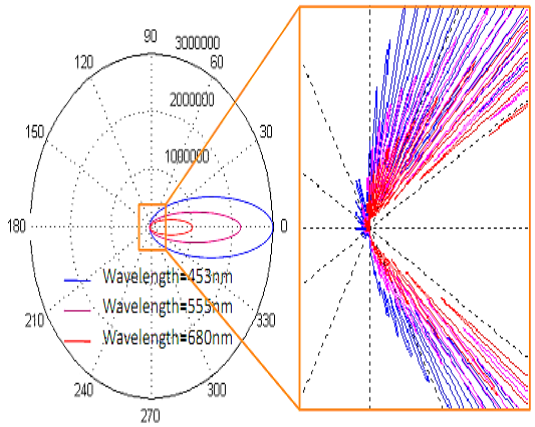

Figure 5. The angular scattering amplitudes of $CaMgSi_2O_6:Eu^{2+},Mn^{2+}$of 453nm, 555nm, and 680nm wavelengths

The discrepancy in CRI values between the SRPS and DRPS shown in Figure 6 is negligible. When increasing the concentration of $CaMgSi_2O_6:Eu^{2+},Mn^{2+}$up to 22%, CRI of SRPS and DRPS tend to climb up, especially with the highest ACCT at 8500 K, which have an important meaning in improving CRI for both SRPS and DRPS. While CRI is hard to control at high ACCT (8500 K), phosphor $CaMgSi_2O_6:Eu^{2+},Mn^{2+}$can definitely make it possible. However, CRI is just one of the indicators used to evaluate the color quality, which has recently been replaced by a newerquality indicator called CQS.

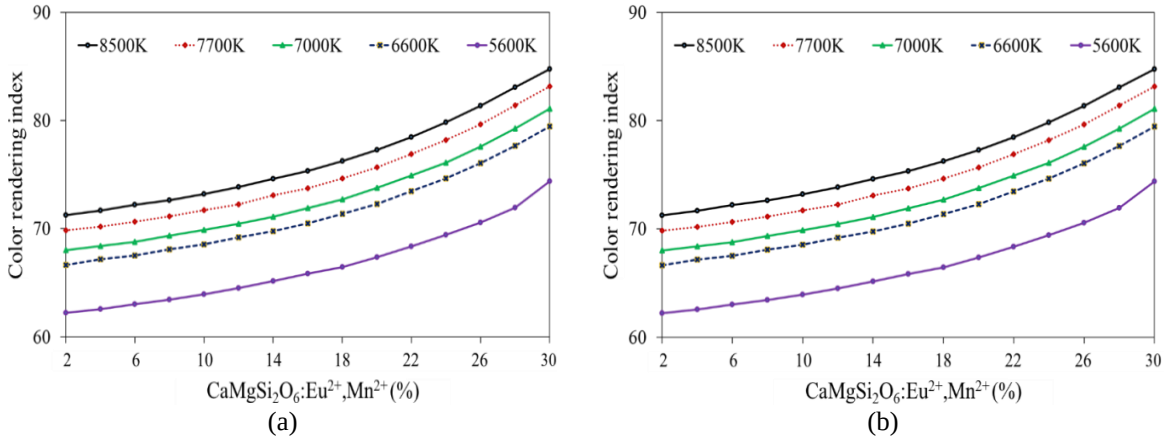

Figure 6. CRI values of SRPS (a) and DRPS (b) grow with $CaMgSi_2O_6:Eu^{2+},Mn^{2+}$concentration

CQS involves three elements: CRI, viewers' preference, and color coordinates, making it becomes the most critical indicator to assess color quality. As known, the CRI value of SRPS continues to increase when $CaMgSi_2O_6:Eu^{2+},Mn^{2+}$concentration exceeds 30% while the CRI value of DRPS has a tendency to drop at all ACCTs after this concentration limit. This is the same to CQS as the results ofSRPS and DRPS CQS interactions with $CaMgSi_2O_6:Eu^{2+},Mn^{2+}$concentrationare shown in Figure 7. SRPS can yield the highest CQS of 71 at CCT 8500K while 74 is the highest CQS value of DRPS at most ACCTs. Thus, it can be concluded that DRPS brings greater color quality than SRPS.As illustrated in Figure 6 and Figure 7, CRI and CQS go up sharply when the red phosphor concentration is adjusted in the range of 2% - 30 %. The greatest value of CRI and CQS were respectively 85 and 71 at 30% $CaMgSi_2O_6:Eu^{2+}$,Mn concentration while the highest angular scattering amplitudes of $CaMgSi_2O_6:Eu^{2+}$,Mn is achieved at 453 nm wavelength as mentioned in Figure 5, which means the blue-light scattering is benefited from the added $CaMgSi_2O_6:Eu^{2+}$,Mn concentration as well, bringing not only advantages for chromatic performance improvements but also light output. The backscattering event, however, will occur in SFPS if $CaMgSi_2O_6:Eu^{2+}$,Mn concentration exceeds 14% causinglight loss and resulting in reduced luminous flux which can be observed from the lumen output values of SRPS and DRPS expressed in Figure 8.

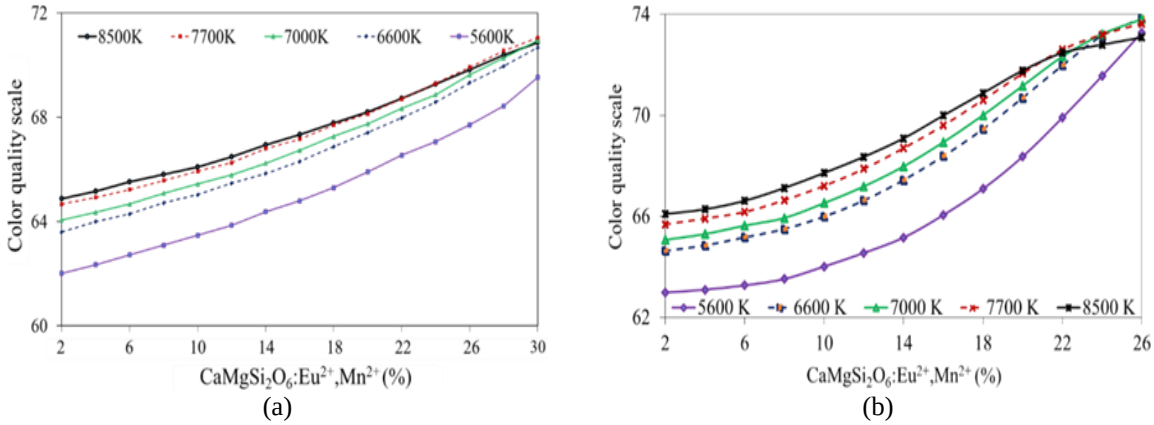

Figure 7. CQS values of SRPS (a) and DRPS (b) grow with $CaMgSi_2O_6:Eu^{2+},Mn^{2+}$concentration

As a result, the luminous flux increases sharply at first, then reaches the peak value and finally goes down slightly, as depicted in Figure 8 (a). Figure 8 (b) depicted a sharp reduction in DRPS brightness when increasing the concentration of red phosphor $CaMgSi_2O_6:Eu^{2+},Mn^{2+}$, which is the result of a noticeable decrease in energy from transmitting light through the red phosphor layer. However, at 2-14% $CaMgSi_2O_6:Eu^{2+},Mn^{2+}$, luminous flux of DRPS is always greater than SRPS at all ACCTs. Therefore, DRPS provides both higher brightness and CQS for WLEDs than SRPS.

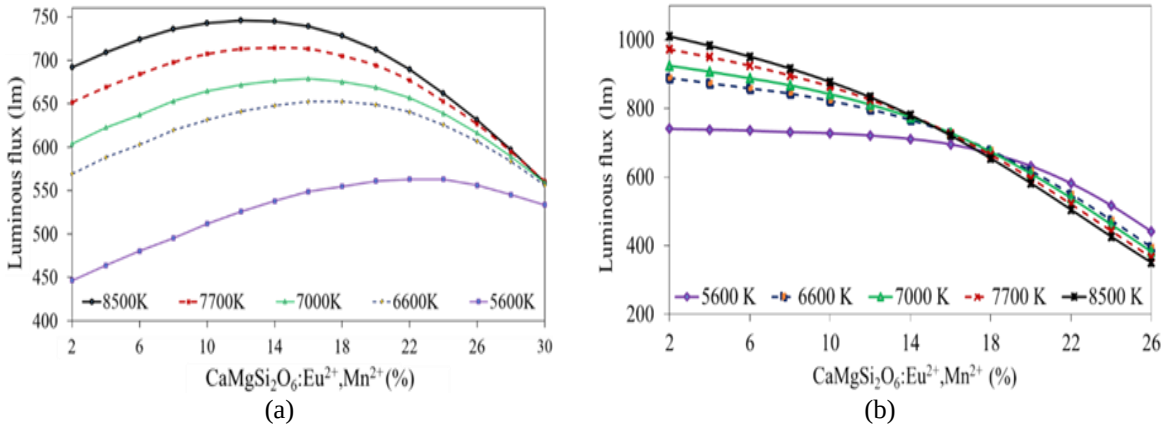

Figure 8. Lumen outputs of SRPS (a) and DRPS (b) with $CaMgSi_2O_6:Eu^{2+},Mn^{2+}$concentration

5. CONCLUSION

To sum up, this study has focused on solving two problems: (1) comparing CQS and LED optical performance of SRPS and DRPS, and (2) analyzing the effect of red phosphor $CaMgSi_2O_6:Eu^{2+},Mn^{2+}$ on CQS and LF of these two structures. Both phosphor structure and phosphor concentration should be simultaneously modified till an appropriate value to achieve the desired CQS and LE. The results showed that CRI and CQS go up when raising the $CaMgSi_2O_6:Eu^{2+},Mn^{2+}$ concentration. DRPS yields a CQS of 74 at ACCTs ranging from 5600K to 8500K but it causes a significant decrease in LF. However, this structure always brings higher luminous flux than SRPS does at all ACCTs with about 2-14% of $CaMgSi_2O_6:Eu^{2+},Mn^{2+}$. This result is demonstrated through the scattering properties of $CaMgSi_2O_6:Eu^{2+},Mn^{2+}$ including the scattering coefficient $\mu_{sca}(\lambda)$, anisotropy factor $g(\lambda)$, reduced scattering coefficient $\delta_{sca}(\lambda)$, and the angular scattering amplitudes $S_1(\theta)$ and $S_2(\theta)$. In conclusion, the CRI of SRPS and DRPS are almost equivalent while the CQS and LF of DRPS outperform that of the SRPS. Therefore, the concentration of $CaMgSi_2O_6:Eu^{2+},Mn^{2+}$ must be selected appropriately to achieve the desired CQS and LF.

REFERENCES

[1] Z. Guo, et al., "Spectral optimization of candle-like white light-emitting diodes with high color rendering index and luminous efficacy," *Journal of Display Technology*, vol. 12, no. 11, pp. 1393-1397, 2016.
[2] P. J. Pedro, et al., "Unique hue correction applied to the color rendering of LED light sources," *Journal of the Optical Society of America*, vol. 33, no. 3, pp. A248-A254, 2016.
[3] G. He, et al., "Study on the correlations between color rendering indices and the spectral power distributions: comment," *Optics Express*, vol. 23, no. 3, pp. A140-A145, 2015.
[4] David, et al., "Development of the IES method for evaluating the color rendition of light sources," *Optics Express*, vol. 23, no. 12, pp. 15888-15906, 2015.
[5] L. Y. Chen, et al., "Chromaticity tailorable glass-based phosphor-converted white light-emitting diodes with high color rendering index," *Optics Express*, vol. 23, no. 15, pp. A1024-A1029, 2015.
[6] J. K. Sheu, et al., "Warm-white light-emitting diode with high color rendering index fabricated by combining trichromatic InGaN emitter with single red phosphor," *Optics Express*, vol. 23, no. 7, pp. A232-A239, 2015.
[7] Y. Yuan, et al., "Excellent color rendering index and high quantum efficiency of rare-earth-free fluosilicate glass for single-phase white light phosphor," *Optics Letters*, vol. 41, no. 13, pp. 3122-3125, 2016.
[8] M. T. Wang, and J. M. Huang, "Accurate control of chromaticity and spectra by feedback phosphor coating," *Optics Express*, vol. 23, no. 9, pp. 11576-11585, 2015.
[9] Y. Lin, Z. Guo, and Y. Cao, "Study on the correlations between color rendering indices and the spectral power distributions: reply to comment," *Optics Express*, vol. 23, no. 3, pp. A146-A148, 2015.
[10] W. G. Bi, et al., "Improved efficacy of warm-white light-emitting diode luminaires," *Applied Optics*, vol. 54, no. 6, pp. 1320-1325, 2015.
[11] K. Y. Yeh, et al., "Novel blue-emitting phosphors - $BaBeSiO_4:Eu^{2+}$: luminescence properties and its application for UV-light emitting diodes," *Optical Materials Express*, vol. 6, no. 2, pp. 416-428, 2016.
[12] S. P. Ying, and J. Y. Shen, "Concentric ring phosphor geometry on the luminous efficiency of white-light-emitting diodes with excellent color rendering property," *Optics Letters*, vol. 41, no. 9, pp. 1989-9192, 2016.
[13] J. Kaur, et al., "UV induced thermoluminescence and photoluminescence studies of Sm3+ Doped LaAlO3 phosphor," *Journal of Display Technology*, vol. 12, no. 9, pp. 928-932, 2016.

[14] J. Xu, J. Ueda, and S. Tanabe, "Design of deep-red persistent phosphors of $Gd_3Al_{5-x}Ga_xO_{12}:Cr^{3+}$ transparent ceramics sensitized by Eu^{3+} as an electron trap using conduction band engineering," *Optical Materials Express*, vol. 5, no. 5, pp. 963-968, 2015.
[15] H. Xiao, et al., "Red-phosphor-dot-doped array in mirror-surface substrate light-emitting diodes," *Journal of Display Technology*, vol. 12, no. 8, pp. 873-877, 2016.
[16] O. H. Kwon, et al., "White luminescence characteristics of red/green silicate phosphor-glass thick film layers printed on glass substrate," *Optical Materials Express*, vol. 6, no. 3, pp. 938-945, 2016.
[17] L. Wang, et al., "Highly efficient narrow-band green and red phosphors enabling wider color-gamut LED backlight for more brilliant displays," *Optics Express*, vol. 23, no. 22, pp. 28707-28717, 2015.
[18] Y. Du, et al., "Electroluminescent properties of WLEDs with the structures of Ce:YAG single crystal/blue chip and $Sr_2Si_5N_8:Eu^{2+}$Ce:YAG single crystal/blue chip," *Journal of Display Technology*, vol. 12, no. 4, pp. 323-327, 2016.
[19] J. W. Moon, et al., "Optical characteristics and longevity of the line-emitting K2SiF6:Mn4+ phosphor for LED application," *Optical Materials Express*, vol. 6, no. 3, pp. 782-792, 2016.
[20] Liu, et al., "Red-blue-green solid state light sources using a narrow line-width green phosphor," *Optics Express*, vol. 23, no. 7, pp. A309-A315, 2015.
[21] V. K. Rai, and A. Pandey, "Efficient color tunable $ZnWO_4:Er^{3+}$-Yb^{3+} phosphor for high temperature sensing," *Journal of Display Technology*, vol. 12, no. 11, pp. 1472-1477, 2016.
[22] C. Hu, et al., "YAG:Ce/(Gd,Y)AG:Ce dual-layered composite structure ceramic phosphors designed for bright white light-emitting diodes with various CCT," *Optics Express*, vol. 23, no. 14, pp. 18243-18255, 2015.
[23] C. H. Chiang, et al., "Effects of phosphor distribution and step-index remote configuration on the performance of white light-emitting diodes," *Optics Letters*, vol. 40, no. 12, pp. 2830-2833, 2015.
[24] J. Hu, et al., "Near ultraviolet excited Eu^{3+} doped Li3Ba2La3(WO4)8 red phosphors for white light emitting diodes," *Optical Materials Express*, vol. 6, no. 1, pp. 181-190, 2016.
[25] K. Y. Yeh, et al., "Novel blue-emitting phosphors - $BaBeSiO_4:Eu^{2+}$: luminescence properties and its application for UV-light emitting diodes," *Optical Materials Express*, vol. 6, no. 2, pp. 416-428, 2016.